JCS ePress online publication date 18 January 2005

Direct transport across the plasma membrane of mammalian cells of *Leishmania* HASPB as revealed by a CHO export mutant

Carolin Stegmayer[1], Angelika Kehlenbach[2], Stella Tournaviti[1], Sabine Wegehingel[1], Christoph Zehe[1], Paul Denny[3], Deborah F. Smith[3], Blanche Schwappach[2] and Walter Nickel[1,*]

[1]Heidelberg University Biochemistry Center, Im Neuenheimer Feld 328, 69120 Heidelberg, Germany
[2]Zentrum für Molekulare Biologie Heidelberg, 69120 Heidelberg, Germany
[3]Wellcome Trust Laboratories for Molecular Parasitology, Department of Biological Sciences, Imperial College London, SW7 2AZ, UK
*Author for correspondence (e-mail: walter.nickel@urz.uni-heidelberg.de)

Accepted 11 November 2004
Journal of Cell Science 118, 517-527 Published by The Company of Biologists 2005
doi:10.1242/jcs.01645

Summary

***Leishmania* HASPB is a lipoprotein that is exported to the extracellular space from both *Leishmania* parasites and mammalian cells via an unconventional secretory pathway. Exported HASPB remains anchored in the outer leaflet of the plasma membrane mediated by myristate and palmitate residues covalently attached to the N-terminal SH4 domain of HASPB. HASPB targeting to the plasma membrane depends on SH4 acylation that occurs at intracellular membranes. How acylated HASPB is targeted to the plasma membrane and, in particular, the subcellular site of HASPB membrane translocation is unknown. In order to address this issue, we screened for clonal CHO mutants that are incapable of exporting HASPB. A detailed characterization of such a CHO mutant cell line revealed that the expression level of the HASPB reporter molecule is unchanged compared to CHO wild-type cells; that it is both myristoylated and palmitoylated; and that it is mainly localized to the plasma membrane as judged by confocal microscopy and subcellular fractionation. However, based on a quantitative flow cytometry assay and a biochemical biotinylation assay of surface proteins, HASPB transport to the outer leaflet of the plasma membrane is largely reduced in this mutant. From these data, we conclude that the subcellular site of HASPB membrane translocation is the plasma membrane as the reporter molecule accumulates in this location when export is blocked. Thus, these results allow us to define a two-step process of HASPB cell surface biogenesis in which SH4 acylation of HASPB firstly mediates intracellular targeting to the plasma membrane. In a second step, the plasma membrane-resident machinery, which is apparently disrupted in the CHO mutant cell line, mediates membrane translocation of HASPB. Intriguingly, the angiogenic growth factor FGF-2, another protein secreted by unconventional means, is shown to be secreted normally from the HASPB export mutant cell line. These observations demonstrate that the export machinery component defective in the export mutant cell line functions specifically in the HASPB export pathway.**

Key words: *Leishmania* parasites, Surface coat, Hydrophilic acylated surface protein, Acylation, SH4 domain, Cell surface expression, Non-classical protein export, Fibroblast growth factor 2

Introduction

Transport of most secretory proteins to the extracellular space is mediated by the ER/Golgi-dependent secretory pathway (Palade, 1975; Rothman, 1994; Rothman and Wieland, 1996; Nickel et al., 2002). In the case of soluble factors, the principal targeting motifs are N-terminal signal peptides that direct classical secretory proteins to the translocation machinery of the ER (Keenan et al., 2001). However, for a number of soluble factors with defined extracellular functions, it has been demonstrated that ER/Golgi-independent routes of protein secretion exist (Muesch et al., 1990; Rubartelli and Sitia, 1991; Cleves, 1997; Hughes, 1999; Nickel, 2003; Prudovsky et al., 2003). Among these, the most prominent examples are the angiogenic growth factors FGF-1 (Jackson et al., 1992; Jackson et al., 1995; Shin et al., 1996; LaVallee et al., 1998; Tarantini et al., 1998; Landriscina et al., 2001a; Landriscina et al., 2001b; Prudovsky et al., 2002; Mandinova et al., 2003) and FGF-2 (Mignatti and Rifkin, 1991; Mignatti et al., 1992; Florkiewicz et al., 1995; Trudel et al., 2000; Engling et al., 2002), cytokines like interleukin 1β (IL1β) (Rubartelli et al., 1990; Andrei et al., 1999; Andrei et al., 2004) and migration inhibitory factor (MIF) (Flieger et al., 2003) as well as the galectin protein family, lectins of the extracellular matrix (Cooper and Barondes, 1990; Cleves et al., 1996; Lutomski et al., 1997). These and other unconventional secretory proteins are characterized by the lack of a signal peptide, by not being glycosylated (despite bearing multiple consensus sites for this post-translational modification) and, most importantly, by an export mechanism that is fully functional in the presence of brefeldin A (Cleves, 1997; Hughes, 1999; Nickel, 2003), a drug that blocks ER/Golgi-dependent protein transport (Misumi et al., 1986; Lippincott-Schwartz et al., 1989; Orci et al., 1991).

Leishmania HASPB is another interesting kind of unconventional secretory protein that is a component of the surface coat of *Leishmania* parasites (Flinn et al., 1994; McKean et al., 1997; Alce et al., 1999). HASPB is exclusively expressed in infective parasites in both extracellular metacyclics and intracellular amastigotes of *L. major* and *L. donovani* (Rangarajan et al., 1995; McKean et al., 1997; Alce et al., 1999) suggesting a role in parasite virulence, although gene deletion mutants retain their viability in the host (McKean et al., 2001). Intriguingly, following heterologous expression, HASPB is also externalized by mammalian cells (Denny et al., 2000) suggesting that endogenous factors exist in higher eukaryotes that are exported in a mechanistically similar manner.

HASPB contains an N-terminal SH4 domain that becomes dually acylated by myristoylation of glycine 2 and palmitoylation of cysteine 5 (Denny et al., 2000). These post-translational modifications are essential for HASPB targeting to the cell surface of *Leishmania* parasites (Pimenta et al., 1994; Denny et al., 2000). Interestingly, the extreme N-terminus of HASPB (HASPB-N18) is sufficient for targeting of HASPB-N18-GFP to the cell surface (Denny et al., 2000). A myristoylated HASPB mutant that cannot be palmitoylated ($HASPB^{C5S}$-GFP) has been found to localize to Golgi membranes (Denny et al., 2000) suggesting that HASPB associates at least transiently with membranes of the classical secretory pathway. Therefore, even though palmitoylacyltransferase activities have not only been localized to the Golgi but also to the ER and plasma membranes (reviewed by Bijlmakers and Marsh, 2003), it is likely that transfer of palmitate to the SH4 domain of HASPB occurs at the Golgi. Following palmitoylation, HASPB is transferred to the plasma membrane but the mechanism of this transport process is unknown. Interestingly, HASPB surface expression in mammalian cells is not affected by brefeldin A (Denny et al., 2000), making it unlikely that dually acylated HASPB reaches the plasma membrane bound to the cytoplasmic leaflet of secretory vesicles. Based on these considerations, HASPB trafficking appears to be distinct from all three known classes of plasma membrane-targeted proteins carrying dual acylation motifs at their N-termini (Bijlmakers and Marsh, 2003). The first of these, the Src kinase Lck, is palmitoylated at the Golgi followed by brefeldin A-sensitive transport to the plasma membrane (Bijlmakers and Marsh, 1999; Bijlmakers and Marsh, 2003). Secondly, $G\alpha_\zeta$ subunits of plasma membrane-resident trimeric G proteins are transiently associated with intracellular membranes like Lck, but these factors get palmitoylated at the plasma membrane and transport to this site is fully operational in the presence of brefeldin A (Fishburn et al., 1999; Bijlmakers and Marsh, 2003). Finally, a third mechanism of plasma membrane targeting of N-terminally acylated proteins is exemplified by the Src kinase Fyn that does not appear to contact intracellular membranes but rather is directly targeted from the cytoplasm to the plasma membrane. Consistently, brefeldin A does not affect Fyn targeting (van't Hof and Resh, 1997; Bijlmakers and Marsh, 2003). As indicated above, current knowledge about HASPB targeting to the plasma membrane does not fit with any of these examples as HASPB is transiently associated with, and most likely palmitoylated at, the Golgi followed by plasma membrane targeting in a brefeldin A-insensitive manner (Denny et al., 2000).

Based on these considerations, many questions about the molecular mechanism of HASPB targeting to the plasma membrane remain unresolved. There is also a complete lack of knowledge about the subcellular site of membrane translocation of HASPB, a process that eventually allows HASPB exposure on the cell surface of eukaryotic cells. In the current study, we introduce a novel experimental system that permits the precise quantification of HASPB export from mammalian cells based on flow cytometry. Using this assay, we screened for somatic CHO mutants that are incapable of exporting HASPB-GFP fusion protein employing retroviral insertion mutagenesis. Based on a detailed biochemical and morphological characterization of a mutant with this phenotype, we conclude that the site of HASPB membrane translocation is the plasma membrane. These data suggest that in the CHO mutant described, a component of a plasma membrane-resident machinery has been disrupted causing the fully acylated HASPB-GFP reporter molecule to accumulate in the inner leaflet of the plasma membrane. These results support a two-step process of HASPB biogenesis, in which dual acylation of the HASPB SH4 domain is required for delivery to the inner leaflet of the plasma membrane and subsequent recognition by a putative translocation machinery. Intriguingly, the component of the HASPB export apparatus that has been disrupted in the mutant cell line appears to be specific for this export pathway, as the angiogenic growth factor FGF-2, another protein secreted by unconventional means, is found to be exported normally from the HASPB export mutant cell line.

Materials and Methods

Antibodies

Affinity-purified anti-GFP antibodies were generated as described earlier (Engling et al., 2002; Seelenmeyer et al., 2003). Antibodies directed against the transferrin receptor were from Zymed, antibodies directed against GM130 were purchased from BD Transduction Laboratories. Monoclonal anti-CD4 antibodies were obtained from cell culture supernatants of the hybridoma cell line Okt4 (ATCC CRL-8002). APC-conjugated anti-rabbit and anti-mouse IgG antibodies used for FACS analyses were from Molecular Probes.

Generation of HASPB-GFP fusion protein expressing cell lines

All HASPB fusion proteins used in this study are based on enhanced GFP (Clontech). The 18 N-terminal amino acids of HASPB (MGSSCTKDSAKEPQKRAD) were fused to the N-terminus of eGFP through a short linker sequence (GPVAT). In case of HASPB-N18-GFP Δmyr/palm and HASPB-N18-GFP Δpalm, two single amino acid changes were introduced to prevent myristoylation and palmitoylation (G2A), and palmitoylation (C5S), respectively. All constructs were cloned into the retroviral expression vector pREV-TRE2 that contains a doxicycline-dependent promoter. Generation of CHO cell lines expressing the various HASPB fusion proteins employing retroviral transduction was performed as described previously (Engling et al., 2002).

Biochemical analysis of membrane association of HASPB-GFP fusion proteins

CHO cells expressing the various kinds of HASPB-GFP fusion proteins were cultured for 2 days at 37°C in the presence of doxicycline (1 μg/ml). Following detachment using PBS/EDTA, cells were collected by centrifugation (500 ***g***, 5 minutes) and resuspended in PBS/sucrose (10% w/w) homogenization buffer. Cells were broken up

by sonication and then ultracentrifuged for 60 minutes at 100,000 ***g***. The resulting supernatant was defined as the cytosolic fraction, the sediment was resuspended in homogenization buffer and defined as the membrane fraction. For carbonate extraction experiments, membranes were again collected by ultracentrifugation. Following resuspension in Na_2CO_3 (0.1 M, pH 11.5), the samples were incubated for 30 minutes at 4°C. Membranes were re-isolated by ultracentrifugation and separated into supernatant (peripheral membrane proteins) and membrane sediment (integral and tightly associated proteins).

Metabolic labeling of CHO cells using [^{3}H]myristate and [^{3}H]palmitate

CHO cells expressing HASPB-GFP fusion proteins were grown on six-well plates for 48 hours at 37°C in the presence of doxicycline (1 μg/ml) to about 80% confluency. Following 2 hours of incubation in FCS-free medium, cells were incubated in FCS-free medium containing either 250 μCi [^{3}H]palmitic acid or 100 μCi [^{3}H]myristic acid. After 3 hours of incubation in labeling medium at 37°C, cells were washed and lysed in buffer containing detergent by sonication. Following removal of insoluble material by centrifugation (14,000 ***g***, 10 minutes), the lysates were subjected to immunoprecipitation of HASPB-GFP fusion proteins employing affinity-purified anti-GFP antibodies. Antibody-bound protein was eluted with SDS sample buffer and subjected to SDS-PAGE. For this purpose, the samples were split into two fractions in order to analyze the eluted proteins by both fluorography and silver staining. For fluorography, SDS gels were treated with NAMP100 amplifier solution (Amersham) and then dried for exposure using Hyperfilm^{TM} (Amersham). Typically, SDS gels containing [^{3}H]myristic acid-labeled proteins were exposed for about 2 weeks whereas SDS gels containing [^{3}H]palmitic acid-labeled proteins were exposed for up to 6 weeks.

Confocal microscopy

CHO cells expressing HASPB-GFP fusion proteins were grown on glass cover slips for 48 hours at 37°C in the presence of 1 μg/ml doxicyclin. The cells were then processed including paraformaldehyde fixation (3% w/v) for 20 minutes at 4°C. The specimens were mounted in Fluoromount G (Southern Biotechnology Associates) and GFP-derived fluorescence was viewed with a Zeiss LSM 510 confocal microscope.

Fluorescence-activated cell sorting

CHO cells expressing HASPB-GFP fusion proteins were grown under the conditions indicated in the corresponding figure legends. In order to detach the cells from the culture plates without using protease-based protocols, cell dissociation buffer (Life Technologies) was used to generate a cell suspension devoid of cell aggregates. Where indicated, cells were treated with affinity-purified anti-GFP antibodies for 1 hour at 4°C on a rotating wheel. Wash procedures were carried out by sedimenting the cells at 200 ***g*** for 3 minutes at 4°C. Primary antibodies were detected with goat anti-rabbit secondary antibodies coupled to allophycocyanin (APC; Molecular Probes). Prior to FACS analysis, propidium iodide (1 μg/ml) was added in order to detect damaged cells. GFP- and APC-derived fluorescence was analyzed using a Becton Dickinson FACSCalibur flow cytometer. Autofluorescence was determined by measuring non-induced cells that were treated with primary and APC-coupled secondary antibodies. FACS-mediated isolation of cell populations and clones was performed using a Becton Dickinson FACSVantage cell sorter.

Biochemical analysis of cell surface-associated HASPB-GFP fusion proteins

CHO cells expressing HASPB-GFP fusion proteins were grown under the conditions indicated in the corresponding figure legends. Following removal of the medium, the cells were washed twice with PBS containing Ca^{2+} and Mg^{2+} (2 mM each). A membrane-impermeable biotinylation reagent (EZ-Link Sulfo-NHS-SS-biotin; Pierce) dissolved in 10 mM triethanolamine, 150 mM NaCl and 2 mM $CaCl_2$ (pH 9) was added at a final concentration of 1 mg/ml. Following incubation for 30 minutes at 4°C quenching of excess amounts of biotinylation reagent was achieved by adding 100 mM PBS/glycine. The cells were then washed twice with PBS containing 2 mM Ca^{2+} and Mg^{2+}. Cell lysates were prepared by adding PBS containing NP-40. Cell lysates were cleared by centrifugation and biotinylated and non-biotinylated proteins were separated by streptavidin affinity chromatography. The two fractions were probed for the presence of HASPB-GFP fusion proteins using SDS-PAGE and western blotting with affinity-purified anti-GFP antibodies.

Retroviral insertion mutagenesis and FACS-based isolation of HASPB export mutants

To randomly mutate CHO cells, we prepared retroviral particles encoding the cell surface protein CD4 (pBI-CD4) (Liu et al., 2000) using the Viraport system (Stratagene). CHO cells expressing HASPB-N18-GFP were transduced according to standard procedures. Following 3 days of incubation at 37°C CD4-positive cells were selected by FACS sorting. In order to isolate HASPB export mutants CD4-positive cells were subjected to multiple rounds of FACS sorting, selecting for cells with high GFP fluorescence and low cell surface staining. In the third round of FACS sorting, individual cells were collected and further propagated in 96-well plates at 37°C. The corresponding clonal cell lines were then characterized as described.

Results

Generation of model cell lines to study HASPB export from mammalian cells

In order to study the export mechanism of HASPB on a quantitative basis in mammalian cells, we generated CHO cells that express various kinds of HASPB-GFP fusion proteins in a doxicycline-dependent manner. $CHO_{MCAT\text{-}TAM2}$ cells (Engling et al., 2002) were transduced with retroviruses carrying HASPB-N18-GFP, HASPB-N18-GFP-Δpalm (C5S), HASPB-N18-GFP-Δmyr/palm (G2A) or GFP, respectively. Clonal cell lines were obtained by several rounds of FACS sorting in the absence and presence of doxicycline, respectively, followed by the selection of single cells characterized by GFP-derived fluorescence only after the addition of doxicycline. As shown in Fig. 1A, expression of the various reporter molecules could only be detected following incubation of the cells with doxicycline as analyzed by western blotting employing anti-GFP antibodies.

Characterization of HASPB fusion protein-expressing model cell lines

We then tested the overall membrane association of the various HASPB fusion proteins by subcellular fractionation into a soluble pool (referred to as ‘cytosol’; Fig. 1B, lane 1) and a membrane fraction (Fig. 1B, lane 2). Additionally, the membrane fraction was subjected to carbonate extraction (Fujiki et al., 1982) to discriminate loosely attached material (Fig. 1B, lane 3) from protein tightly associated with membranes (Fig. 1B, lane 4). Typically roughly equal amounts of HASPB-N18-GFP were found in the cytosolic and the

membrane fractions. About two thirds of the membrane-bound material was found to be resistant to carbonate treatment. In the case of HASPB-N18-GFP-Δpalm (C5S), as expected, the population found in the cytosolic fraction was significantly larger than that present in the membrane fraction (Fig. 1B). About 50% of membrane-associated HASPB-N18-GFP-Δpalm was found to be resistant to carbonate treatment. The vast majority of HASPB-N18-GFP-Δmyr/palm (G2A), a mutant that lacks both myristoylation and palmitoylation, was found in the cytosolic fraction which is also the case for GFP lacking the HASPB-N18 sequence (Fig. 1B). Thus, subcellular fractionation combined with carbonate extraction allows analysis of the acylation status of HASPB fusion proteins.

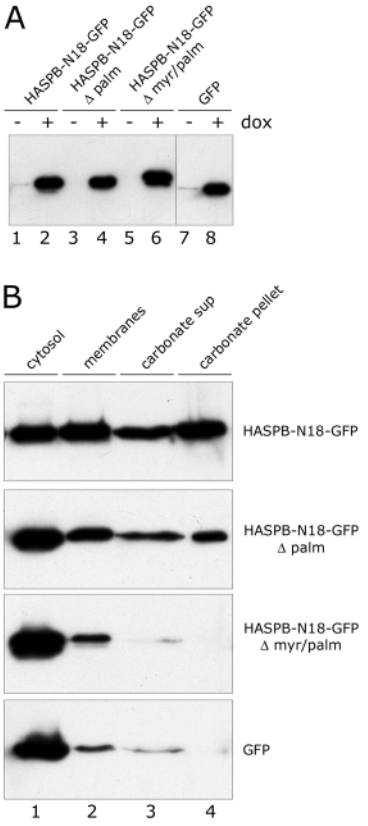

Fig. 1. Expression level and membrane association of HASPB-GFP fusion proteins expressed in CHO cells. (A) CHO cells expressing HASPB-GFP fusion proteins as indicated were grown on six-well plates in the absence (lanes 1, 3, 5 and 7) or presence (lanes 2, 4, 6 and 8) of 1 μg/ml doxicycline (dox). Cells were detached and collected by centrifugation followed by lysis in SDS sample buffer. 1% of each lysate corresponding to cells from one well were subjected to SDS-PAGE. Following SDS-PAGE and western blotting HASPB-GFP fusion proteins were detected using affinity-purified anti-GFP antibodies. (B) CHO cells expressing HASPB-GFP fusion proteins as indicated were fractionated into cytosolic (lane 1) and membrane fractions (lane 2). Additionally, the membrane fraction was subjected to carbonate extraction resulting in a carbonate supernatant containing loosely bound proteins (lane 3) and a carbonate pellet containing proteins tightly associated with membranes (lane 4). 5% of each fraction was combined with SDS sample buffer and proteins were separated by SDS-PAGE. Following western blotting, HASPB-GFP fusion proteins were detected with affinity-purified anti-GFP antibodies.

We next analyzed the subcellular distribution of the HASPB-GFP fusion proteins employing confocal microscopy (Fig. 2). HASPB-N18-GFP was found to localize mainly to the plasma membrane as well as to droplet-like structures that were typically located in close proximity to the plasma membrane (Fig. 2A). By contrast, HASPB-N18-GFP-Δpalm was not at all associated with the plasma membrane but was rather localized on intracellular membranes in a perinuclear position (Fig. 2B). As expected, HASPB-N18-GFP-Δmyr/palm was found exclusively in the cytoplasm (Fig. 2C) with a staining pattern indistinguishable from that of GFP (Fig. 2D). Thus, membrane association of HASPB-GFP is completely dependent on dual acylation of the HASPB N-terminus. These results are consistent with previous studies analyzing similar constructs in *Leishmania* parasites (Denny et al., 2000).

Functional analysis of HASPB export from CHO cells based on quantitative flow cytometry

Based on previous observations (Denny et al., 2000), an export assay was developed that simultaneously measures both the expression level of a given HASPB-GFP fusion protein and its export to the outer leaflet of the plasma membrane on a quantitative basis. Following membrane translocation, HASPB-GFP fusion proteins remain membrane-anchored through their acylated N-termini, allowing decoration of the extracellular population with anti-GFP antibodies. This subpopulation is then specifically detected using APC-conjugated secondary antibodies. Using flow cytometry, GFP-

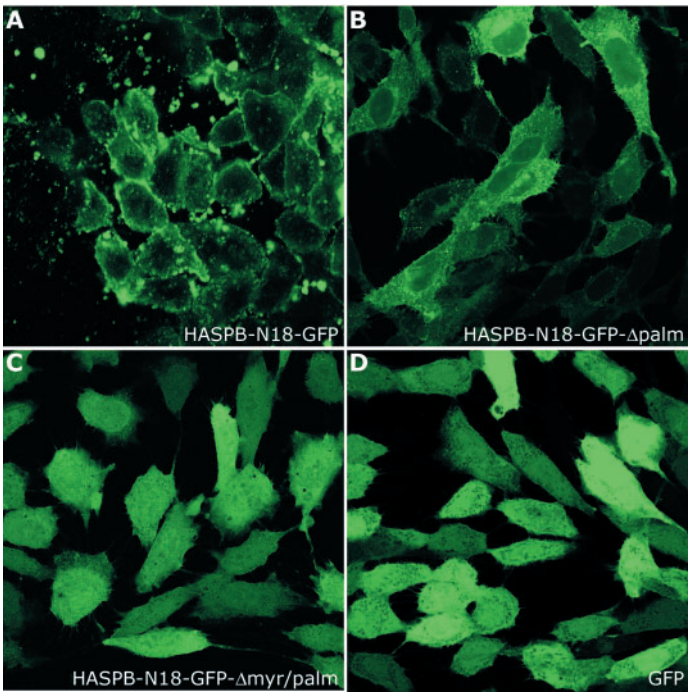

Fig. 2. Subcellular distribution of HASPB-GFP fusion proteins as determined by confocal microscopy. Cells were grown on glass coverslips in the presence of 1 μg/ml doxicycline for 48 hours at 37°C. GFP-derived fluorescence was viewed with a Zeiss LSM 510 confocal microscope. (A) HASPB-N18-GFP; (B) HASPB-N18-GFP-Δpalm; (C) HASPB-N18-GFP-Δmyr/palm; (D) GFP.

derived fluorescence (overall expression level) and APC-derived fluorescence (exported population) is measured simultaneously. All three HASPB-GFP fusion proteins as well as GFP lacking an N-terminal HASPB tag are expressed at similar levels provided that the cells have been treated with doxicycline (Fig. 3A). Only the expression of HASPB-N18-GFP gives rise to surface staining whereas HASPB-N18-GFP-Δpalm, HASPB-N18-GFP-Δpalm/myr and GFP are negative with regard to cell surface staining (Fig. 3B). Again, these data are consistent with previous observations made in parasites (Denny et al., 2000) in that export to the extracellular leaflet of the plasma membrane of mammalian cells is critically dependent on dual acylation of the SH4 N-terminus of HASPB. Thus, the in vivo assay introduced in Fig. 3 allows precise quantification of HASPB export under normalized conditions with respect to the expression level of a given HASPB-GFP fusion protein.

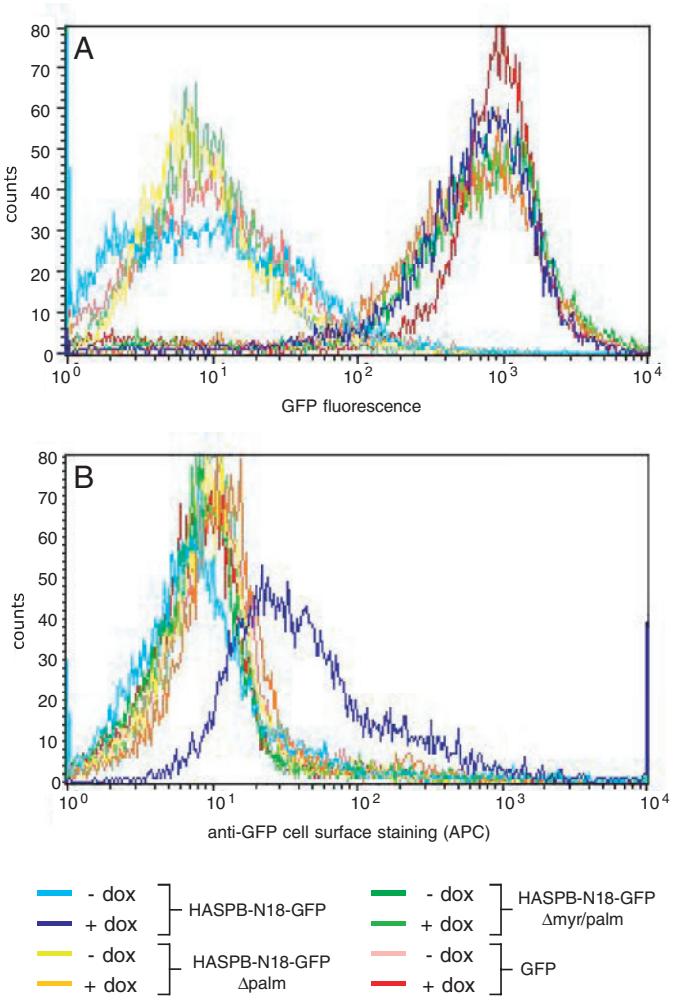

Fig. 3. Quantitative analysis of cell surface localized HASPB-GFP fusion proteins using flow cytometry. (A) GFP-derived fluorescence (expression level). (B) APC-derived fluorescence (cell surface staining). Cells were incubated in the presence or absence of doxicycline as indicated followed by processing for FACS sorting. HASPB-N18-GFP, light and dark blue curves; HASPB-N18-GFP-Δpalm, yellow and orange curves; HASPB-N18-GFP-Δmyr/palm, light and dark green curves; GFP, light and dark red curves.

Biochemical analysis of HASPB-N18-GFP export to the outer leaflet of the plasma membrane of CHO cells

In order to demonstrate an external population of HASPB-N18-GFP associated with the outer leaflet of the plasma membrane using an independent method, biotinylation experiments were carried out employing a membrane-impermeable biotinylation reagent. Cells were incubated in the presence of doxicycline, serum-containing medium was removed followed by treatment with a biotinylation reagent. After quenching and removing excess amounts of the biotinylation reagent, cells were converted into a detergent lysate that was then subjected to streptavidin affinity chromatography to separate biotinylated (cell surface) from non-biotinylated (intracellular) proteins. HASPB-N18-GFP can be detected in the fraction eluted from streptavidin beads (Fig. 4, lane 3) whereas the various controls (HASPB-N18-GFP-Δpalm, HASPB-N18-GFP-Δmyr/palm and GFP) are absent from this fraction. These results demonstrate that the biotinylation reagent does not traverse the plasma membrane and, therefore, the positive signal for HASPB-N18-GFP in the fraction of biotinylated proteins represents a population located on the surface of these cells. Under steady-state conditions, the amount of HASPB-N18-GFP on the surface of CHO cells was calculated by densitometry to vary between experiments within a range of ~3-6% of the overall population (data not shown).

Screening for somatic CHO mutants characterized by a defect in HASPB export

The principal aim of this study was to identify the subcellular

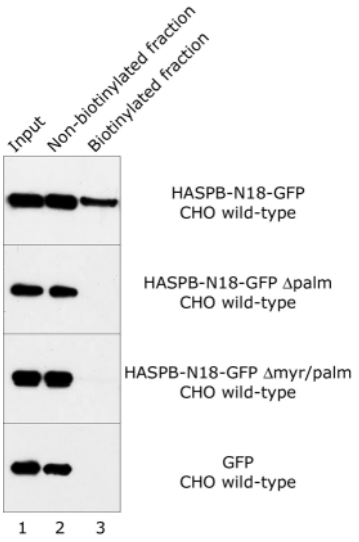

Fig. 4. Biochemical quantification of cell surface localized HASPB-GFP fusion proteins. CHO cells expressing HASPB-GFP fusion proteins as indicated were treated with a membrane-impermeable biotinylation reagent. Cell lysates were generated and biotin-labeled and biotin-unlabeled proteins were separated by streptavidin affinity chromatography. Input material (lane 1; 2%), streptavidin supernatant (non-biotinylated proteins, lane 2; 2%) and streptavidin-bound proteins (biotinylated proteins, lane 3; 50%) were separated on SDS gels followed by western blotting using affinity-purified anti-GFP antibodies.

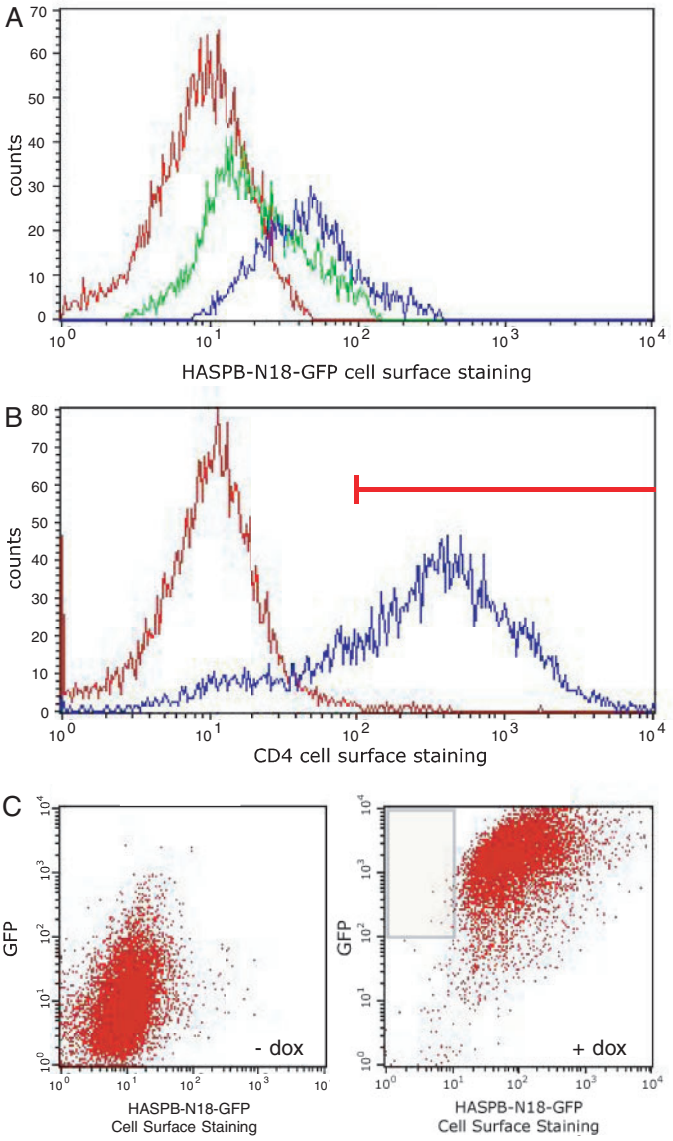

Fig. 5. Retroviral insertion mutagenesis of CHO cells and genetic screening for HASPB export mutants. (A) Intercellular spreading was monitored by growing $CHO_{MCAT\text{-}TAM2}$ cells ('CHO wild type') with $CHO_{MCAT\text{-}TAM2}$ cells retrovirally transduced with the HASPB-N18-GFP construct in a mixed culture. HASPB-N18-GFP expression was induced by 1 μg/ml doxicycline for 48 hours at 37°C. Cells were then processed for FACS sorting using affinity-purified anti-GFP antibodies and APC-coupled secondary antibodies to detect exported HASPB-N18-GFP by cell surface staining. $CHO_{MCAT\text{-}TAM2}$ cells and $CHO_{MCAT\text{-}TAM2}$ cells expressing HASPB-N18-GFP were gated based on GFP fluorescence and APC-derived fluorescence of $CHO_{MCAT\text{-}TAM2}$ cells (green curve) and $CHO_{MCAT\text{-}TAM2}$ cells expressing HASPB-N18-GFP (blue curve) was measured as depicted in the histogram. Autofluorescence was measured using $CHO_{MCAT\text{-}TAM2}$ cells that were treated with antibodies. (B) $CHO_{MCAT\text{-}TAM2}$ cells expressing HASPB-N18-GFP were treated with retroviral particles encoding the cell surface protein CD4. Following transduction, CD4-positive cells were selected based on anti-CD4 cell surface staining using FACS sorting. (C) CD4-positive cells as enriched in the FACS experiment depicted in B were subjected to three rounds of FACS sorting. Cells were monitored in dot blot mode with GFP-derived fluorescence shown on the *y*-axis and HASPB-N18-GFP cell surface staining shown on the *x*-axis. The left-hand panel shows the population grown in the absence of doxicycline, the right-hand panel shows the population grown in the presence of 1 μg/ml doxicycline for 48 hours at 37°C. To select for HASPB export mutants the sorting window was adjusted as depicted in the right-hand panel to isolate cells characterized by high GFP fluorescence and low APC cell surface staining.

site of HASPB membrane translocation in CHO cells. To address this point, we generated clonal CHO mutants by retroviral insertion mutagenesis, which are characterized by a negative HASPB export phenotype. In order to make sure that such mutants can be identified in the presence of wild-type cells, we first conducted experiments designed to detect intercellular spreading of HASPB-N18-GFP following translocation onto the cell surface. For this purpose, HASPB-N18-GFP-expressing and HASPB-N18-GFP-non-expressing cells ($CHO_{MCAT\text{-}TAM2}$) were mixed in culture, treated with doxicycline and subjected to a FACS analysis measuring GFP and APC-derived cell surface fluorescence. Two populations of cells from a mixed culture of $CHO_{MCAT\text{-}TAM2}$ cells (Fig. 5A, green curve) (negative for GFP fluorescence, data not shown) and HASPB-N18-GFP-expressing cells (blue curve) (positive for GFP fluorescence, data not shown) can be easily distinguished by anti-GFP cell surface staining, demonstrating that HASPB-N18-GFP-exporting cells retain the secreted material on their surface. However, cell surface staining of HASPB-N18-GFP-non-expressing cells is in fact significantly higher than the autofluorescence background defined by antibody-treated $CHO_{MCAT\text{-}TAM2}$ cells (Fig. 5A, red curve), suggesting that a certain amount of HASPB-N18-GFP was transferred from HASPB-N18-GFP-expressing cells to non-expressing cells. This observation emphasizes the conclusions drawn from the experiments shown in Figs 3 and 4, in that an extracellular population of HASPB-N18-GFP can be defined by its appearance on the surface of cells that are incapable of expressing the reporter molecule when mixed with HASPB-N18-GFP-expressing cells. With regard to the mutagenesis strategy, however, these experiments demonstrate that HASPB export mutants are distinguishable from wild-type cells on the basis of FACS sorting and can therefore be identified and isolated by this method, even in the presence of a large excess of wild-type cells.

To randomly generate somatic CHO mutants, we chose retroviral insertion mutagenesis. CHO cells carrying the HASPB-N18-GFP reporter gene were transduced with retroviral particles encoding the open reading frame of the integral plasma membrane protein CD4 (Fig. 5B) (Liu et al., 2000). In this context, CD4 was used as a marker for mutated cells that were subsequently enriched by FACS. The pool of CD4-positive mutated cells (Fig. 5B, blue curve) was then subjected to a selection of CHO mutants expressing the HASPB-N18-GFP reporter molecule at a normal level (as compared to wild-type cells) but without localisation to the cell surface. For this purpose, cells were viewed in the FACS set-up in dot blot mode and a sorting window was defined to select for the phenotype described (Fig. 5C). Cells isolated from this window in the first round of sorting (about 0.5% of the total population) were propagated and subjected to a second round of cell sorting in which 3.7% of the selected population displayed the desired phenotype. In a third round of cell

sorting, single cells were selected in the sorting window (defined in Fig. 5C).

Characterization of a clonal CHO mutant cell line defective in HASPB export

In the current study, we provide a detailed characterization of a clonal CHO cell line (from here on referred to as 'K3') derived from the selection procedure of the experiments described in Fig. 5. In order to make sure that the reporter molecule itself does not contain a mutation in the CHO K3 mutant cell line, we isolated genomic DNA and amplified the HASPB-N18-GFP open reading frame. As demonstrated by sequencing of the corresponding PCR product, the sequence of the N-terminal SH4 domain of the reporter molecule was confirmed to be unchanged compared to the parental CHO wild-type cells (data not shown).

Based on GFP-derived fluorescence, the expression level of HASPB-N18-GFP does not significantly differ between wild-type and K3 cells as analyzed by FACS (Fig. 6A). However, HASPB-N18-GFP cell surface staining is largely reduced to about 30% as compared to wild-type levels (Fig. 6A). These data were confirmed by a biochemical assessment of the extracellular population of HASPB-N18-GFP in the wild type compared to K3 mutant cells using the biotinylation assay described in Fig. 4. The amount of biotinylated cell surface HASPB-N18-GFP (Fig. 6B, upper panel; lane 3) derived from K3 cells is reduced to about 20% when compared to CHO wild-type cells (lower panel; lane 3).

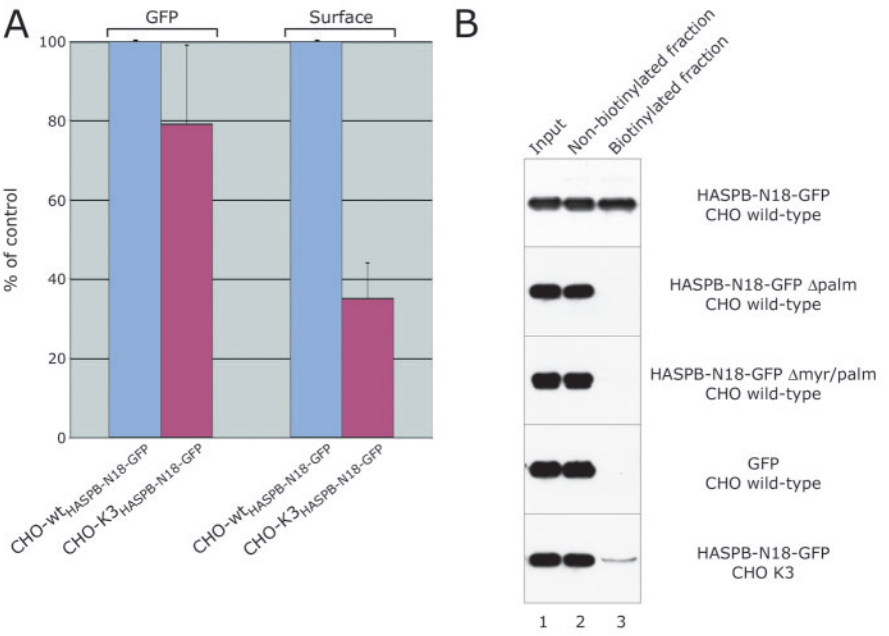

Fig. 6. Characterization of HASPB-N18-GFP export from CHO wild-type cells compared to CHO K3 mutant cells. (A) FACS analysis. CHO wild-type cells and CHO K3 cells were grown for 48 hours at 37°C in the presence of doxicycline (1 μg/ml). Cells were processed for FACS sorting using affinity-purified anti-GFP antibodies and APC-coupled secondary antibodies to detect exported HASPB-N18-GFP by cell surface staining. For a statistical analysis of four independent experiments, GFP-derived fluorescence and APC-derived cell surface staining of CHO wild-type cells expressing HASPB-N18-GFP was set to 100%, respectively. (B) Biochemical analysis of exported HASPB-N18-GFP in CHO wild-type cells, CHO K3 cells and various control cell lines introduced in Figs 1-4 using cell surface biotinylation. The experiment was conducted exactly as described in the Materials and Methods and in the legend to Fig. 4. Input material (lane 1; 2%), streptavidin supernatant (non-biotinylated proteins, lane 2; 2%) and streptavidin-bound proteins (biotinylated proteins, lane 3; 50%) were separated on SDS gels followed by western blotting using affinity-purified anti-GFP antibodies.

As dual acylation of HASPB-N18-GFP is a critical determinant for plasma membrane targeting and export, it was important to analyze whether the reporter molecule HASPB-N18-GFP itself is properly modified in CHO K3 cells. Therefore, in a first set of experiments, overall membrane association of HASPB-N18-GFP was tested in CHO K3 cells by a carbonate extraction analysis. The input material of HASPB-N18-GFP was comparable in wild-type CHO and K3 cells, which is consistent with the FACS experiments shown in Fig. 6, demonstrating that the expression level of HASPB-N18-GFP does not differ significantly in the two cell lines (Fig. 7A). Similarly, there are no apparent differences in the distribution of HASPB-N18-GFP between cytosol and membranes when CHO wild-type and K3 cells are compared (Fig. 7B, lanes 1 and 2). Finally, when the membrane fractions of wild-type and K3 cells were subjected to carbonate extraction, the distribution of HASPB-N18-GFP between the membrane-associated and the soluble pool was identical between the two cell types (Fig. 7B, lanes 3 and 4). These data suggest that the acylation status of HASPB-N18-GFP does not differ between CHO wild-type and K3 cells. This conclusion was confirmed by metabolic labeling of HASPB-N18-GFP in wild-type and K3 cells using [^{3}H]-labeled myristate and [^{3}H]-labeled palmitate. Incorporation of both fatty acids into HASPB-N18-GFP can be detected in both wild-type and K3 cells whereas the corresponding negative controls are either labeled only with [^{3}H]myristate (in the case of HASPB-N18-GFP-Δpalm) or not labeled at all (for HASPB-N18-GFP-Δmyr/palm and GFP) (Fig. 7C). These experiments demonstrate that HASPB-N18-GFP processing in terms of acylation occurs normally in the CHO K3 mutant cell line and, therefore, the lack of HASPB-N18-GFP present on the cell surface of these cells must be due to the translocation machinery itself from which at least one component is apparently disrupted in K3 cells.

HASPB-N18-GFP localizes to the plasma membrane in CHO K3 cells

In order to define the subcellular site of HASPB-N18-GFP membrane translocation, we analyzed its localization in CHO wild-type cells versus CHO K3 cells using confocal microscopy and subcellular fractionation. There was virtually no difference in the subcellular distribution of HASPB-N18-GFP in the two cell types and in both cases the majority of the material is localized to the plasma membrane (Fig. 8A,B).

These morphological data could be confirmed by a biochemical analysis employing subcellular fractionation (Fig. 8C). A protocol to purify plasma membrane vesicles (Schäfer et al., 2004) was used to compare the enrichment of the HASPB-N18-GFP reporter molecule in plasma membranes of CHO wild-type cells (Fig. 8C, lanes 1-4) and CHO K3 cells (Fig. 8C, lanes 5-8), respectively. When compared to the homogenate (lanes 1), HASPB-N18-GFP (lane 5) was found to be enriched in gradient-purified plasma membrane vesicles using the plasma membrane marker transferrin receptor (TfR) (Futter et al., 1998) in both CHO wild-type and CHO K3 cells (lanes 4 and 8, respectively). Using the Golgi marker GM130 (Nakamura et al., 1995), the plasma membrane vesicle fraction was depleted of Golgi membranes demonstrating the significance of the findings described above. The association of HASPB-N18-GFP with plasma membranes in both CHO wild-type cells and K3 cells is considered to be quite striking as it demonstrates a defect in CHO K3 cells directly in the translocation machinery rather than some kind of intracellular segregation of HASPB-N18-GFP that prevents access to the site of membrane translocation. Thus, the HASPB-N18-GFP translocation apparatus is a plasma membrane-resident machinery.

A FGF-2-GFP reporter molecule is exported from CHO wild-type and K3 mutant cells at similar levels

In order to analyze whether the disrupted export component in CHO K3 cells is a specific factor for HASPB export or rather a general component for non-classical secretory processes, we tested whether FGF-2, as a classical example for unconventional secretory proteins (Nickel, 2003), is exported from CHO K3 cells. For this purpose, we transduced both CHO K3 and the parental CHO wild-type cells expressing the HASPB-N18-GFP fusion protein with retroviral particles encoding a FGF-2-GFP fusion protein (Engling et al., 2002; Backhaus et al., 2004). Owing to the different molecular weights (25 and 45 kDa, respectively), the two reporter molecules could be easily distinguished in the cell surface biotinylation assay (Figs 4 and 6). There was no difference in FGF-2 cell surface expression between CHO wild-type and CHO K3 cells (Fig. 9, compare lanes 3 and 6; upper panels), respectively. By contrast, HASPB-N18-GFP analyzed from the same cell preparations is exported only from CHO wild-type cells (compare lanes 3 and 6; lower panels). These results demonstrate that the component disrupted in CHO K3 cells is a specific machinery molecule of the HASPB export pathway.

Discussion

The specific aim of this study was to develop an experimental approach designed to identify the subcellular membrane

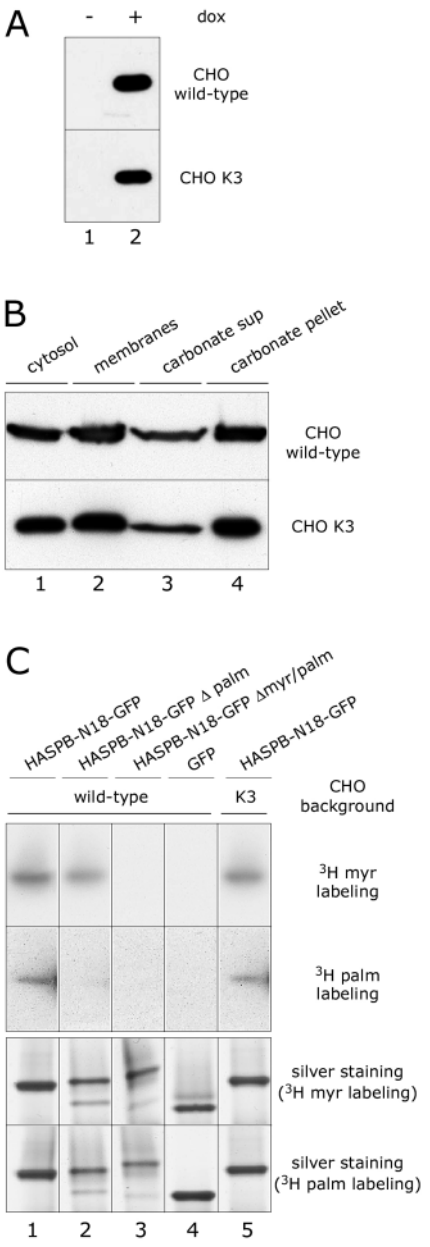

Fig. 7. Expression level, membrane association and post-translational acylation of HASPB-N18-GFP in CHO wild-type cells and CHO mutant K3 cells. (A) CHO wild-type cells and CHO K3 cells (both expressing HASPB-N18-GFP) were grown on six-well plates to about 80% confluency in the absence (lane 1) or presence (lane 2) of doxicycline (1 μg/ml) for 48 hours at 37°C. Cells were detached with PBS/EDTA, collected by centrifugation and lysed in SDS sample buffer. 1% of each lysate corresponding to cells from one well were subjected to SDS-PAGE. HASPB-N18-GFP was detected by western blotting using affinity-purified anti-GFP antibodies. (B) CHO wild-type cells and CHO K3 cells (both expressing HASPB-N18-GFP) were grown on six-well plates to about 80% confluency in the presence of 1 μg/ml doxicycline for 48 hours at 37°C. Subcellular fractionation and carbonate extraction of membranes was performed and 5% of each fraction was combined with SDS sample buffer and proteins were separated by SDS-PAGE. Following western blotting, HASPB-GFP fusion proteins were detected with affinity-purified anti-GFP antibodies. (C) CHO wild-type cells, CHO K3 cells (both expressing HASPB-N18-GFP) as well as control cell lines expressing HASPB-N18-GFP Δmyr/palm and HASPB-N18-GFP Δpalm, respectively, were grown on six-well plates to about 80% confluency in the presence of 1 μg/ml doxicycline for 48 hours at 37°C and labelled with [^{3}H]myristate and [^{3}H]palmitate. Cell lysates were prepared and subjected to immunoprecipitation using affinity-purified anti-GFP antibodies. Immunopurified fractions were split into two samples, separated on SDS gels and either processed by fluorography (upper panel) or silver staining (lower panel).

system that contains the molecular machinery required for cell surface expression of *Leishmania* HASPB in mammalian cells. This question is of general interest because, during its biogenesis, HASPB has been shown to contact intracellular membranes such as the Golgi (Denny et al., 2000). Based on the evidence currently available, the most logical explanation for this observation is that Golgi membranes contain the palmitoylacyltransferase required for the thioester-based acylation of cysteine 5 in the N-terminal SH4 domain of HASPB. From this point on, it is not clear whether fully acylated HASPB translocates across the membrane of the Golgi or whether it is first transported to the plasma membrane associated with the cytoplasmic leaflet of secretory vesicles. Even though overall cell surface expression of HASPB has been shown not to be affected by brefeldin A (Denny et al., 2000), this result does not unequivocally rule out the possibility that HASPB is traveling to the plasma membrane associated with the cytoplasmic leaflet of TGN-derived secretory vesicles. It is also possible that transfer to the plasma membrane involves an intermediate step in which HASPB is not at all associated with intracellular membranes or HASPB might be transported from the TGN to the endosomal system from where it might get access to the plasma membrane.

Based on the uncertainties discussed above, we were interested in establishing an experimental system that allows for a quantitative analysis of HASPB cell surface expression under conditions where defined steps in HASPB biogenesis are blocked. In particular, we were looking for experimental conditions where dual acylation of the N-terminal SH4 domain of HASPB occurs normally but HASPB export to the outer leaflet of the plasma membrane is blocked. In this context, we decided to use CHO cells as a model system as they are well suited to the generation of random somatic mutants. To

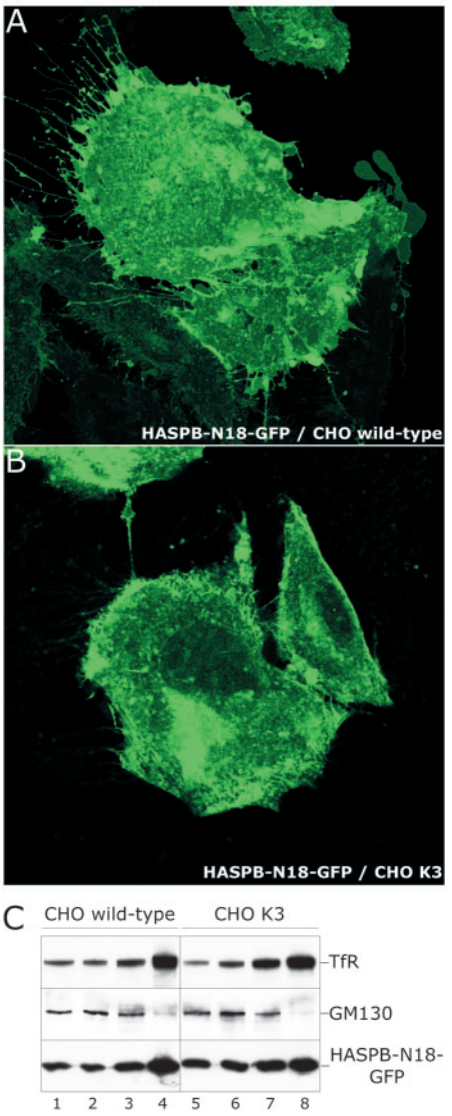

Fig. 8. Subcellular localization of HASPB-N18-GFP in CHO wild-type and CHO K3 mutant cells as determined by confocal microscopy and subcellular fractionation. (A) HASPB-N18-GFP expressed in CHO wild-type cells. (B) HASPB-N18-GFP expressed in CHO K3 mutant cells. Cells were grown on glass coverslips in the presence of 1 μg/ml doxycycline for 48 hours at 37°C and processed for confocal microscopy. GFP-derived fluorescence was viewed with a Zeiss LSM 510 confocal microscope. (C) Subcellular fractionation of CHO wild-type cells and CHO K3 cells was conducted as described earlier (Schäfer et al., 2004). To identify plasma membranes, antibodies directed against the transferrin receptor were used (Futter et al., 1998). To detect Golgi membranes, antibodies directed against GM130 were used (Nakamura et al., 1995). Four fractions were generated and analyzed for each cell line: a hypotonic lysate (lanes 1 and 5), a post-mitochondrial supernatant (lanes 2 and 6), a microsomal membrane fraction (lanes 3 and 7) and gradient-purified plasma membranes (lanes 4 and 8). For each fraction 15 μg total protein were loaded per lane followed by SDS-PAGE and western blotting using the antibodies indicated.

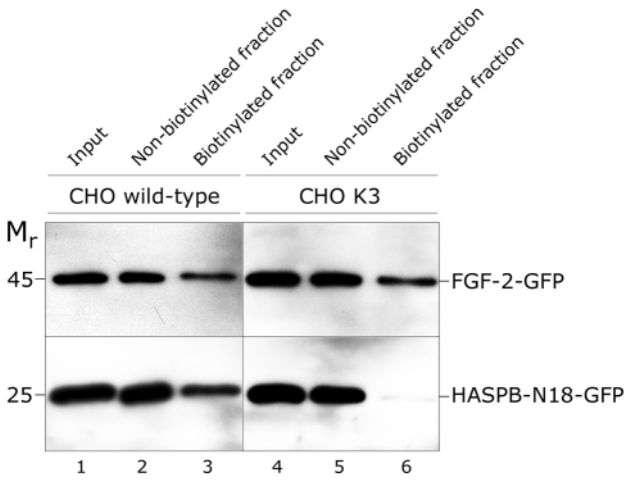

Fig. 9. Secretion of FGF-2 from CHO K3 cells occurs as efficiently as from parental CHO wild-type cells. Parental CHO wild-type (lanes 1-3) and CHO K3 mutant cells (lanes 4-6) expressing HASPB-N18-GFP were transduced with retroviral particles containing the FGF-2-GFP open reading frame controlled by a doxycycline-dependent element. Transduction efficiency was about 65% as determined by GFP-derived fluorescence. Both cell types were treated with a membrane-impermeable biotinylation reagent. Cell lysates were generated and biotin-labeled and biotin-unlabeled proteins were separated by streptavidin affinity chromatography. Input material (lane 1 and 4; 4%), streptavidin supernatant (non-biotinylated proteins, lanes 2 and 5; 4%) and streptavidin-bound proteins (biotinylated proteins, lanes 3 and 6; 50%) were separated on SDS gels followed by western blotting using affinity-purified anti-GFP antibodies.

efficiently mutate CHO cells expressing HASPB-N18-GFP in a doxicycline-dependent manner, we used retroviral insertion mutagenesis with CD4 as a cell surface marker to efficiently enrich mutated cells by FACS. Using the FACS-based experimental system described, we succeeded in isolating clonal CHO mutants with the desired phenotype, one of which has been characterized in detail in the current study.

In the described CHO mutant strain (K3), HASPB-N18-GFP is expressed in a doxicycline-dependent manner at a level comparable to that of wild-type cells. In the context of this work, it was most critical to isolate CHO mutants that do not have any defect in the co- and/or post-translational processing of HASPB, i.e. we were looking for mutants that are still capable of adding both myristate and palmitate to the SH4 domain of HASPB. In the case of CHO K3 cells, this was shown to be the case by carbonate extraction experiments to probe overall membrane association of HASPB-N18-GFP as well as metabolic labeling experiments to demonstrate directly the incorporation of [^{3}H]-labeled myristate and palmitate into HASPB-N18-GFP when expressed in CHO K3 cells. These experiments unequivocally demonstrated that HASPB-N18-GFP is processed normally in CHO K3 mutant cells resulting in a membrane association that is indistinguishable from HASPB-N18-GFP expressed in CHO wild-type cells.

The negative HASPB-N18-GFP export phenotype by which the clonal CHO K3 cell line was isolated could be confirmed by both FACS-based cell surface staining experiments and a biochemical assessment of HASPB-N18-GFP export using a membrane-impermeable biotinylation reagent. Both methods consistently demonstrated that HASPB-N18-GFP cell surface expression in CHO K3 cells is greatly reduced to ~10-30% of the population found on the cell surface of CHO wild-type cells. As the expression level of HASPB-N18-GFP does not differ significantly between CHO K3 and wild-type cells, as shown by both western blotting and GFP-derived fluorescence determined by FACS, we conclude that the process of HASPB-N18-GFP membrane translocation is perturbed in the mutant cell line. Based on this observation, it was then crucial to analyze whether the steady-state distribution of the reporter molecule is changed in CHO K3 cells as compared to wild-type cells. As demonstrated by confocal microscopy and subcellular fractionation, this is not the case as the majority of the HASPB-N18-GFP population localizes in both cell lines to the plasma membrane. Intriguingly, a FGF-2-GFP fusion protein is secreted equally well from the CHO K3 mutant cell line and the parental CHO wild-type cells, demonstrating that the disrupted factor in K3 cells is a specific component of the HASPB export pathway.

From the combined data presented in this study, we conclude that the CHO mutant cell line K3 has a direct defect in the molecular machinery promoting membrane translocation of HASPB. The subcellular distribution of the reporter molecule is unchanged when wild-type and K3 mutants cells are compared, with HASPB-N18-GFP detected in both cases as a plasma membrane-resident protein. As cell surface exposure of the reporter is largely reduced in the mutant cell line, we conclude that the plasma membrane is the subcellular site of membrane translocation of HASPB-N18-GFP. Thus, along with the angiogenic growth factors FGF-1 and FGF-2 (Prudovsky et al., 2002; Schäfer et al., 2004), HASPB represents another example of an unconventional secretory protein that is translocated directly across the plasma membrane of mammalian cells in order to be exposed to the extracellular space. Our data allow us to describe a two-step process for the overall biogenesis of HASPB that is defined by acylation-dependent targeting to the inner leaflet of the plasma membrane followed by translocation across the plasma membrane, resulting in a membrane-anchored lipoprotein on the surface of both parasites and mammalian cells.

The experimental approach presented in this study shows great promise for addressing a number of questions related to HASPB biogenesis in the future. In this regard, our goals are not restricted to the molecular analysis of the HASPB membrane translocation apparatus itself but also concern the preceding steps such as the molecular identity and the exact subcellular localization of the HASPB palmitoylacyltransferase. Moreover, it remains a completely open question how HASPB is transferred from the Golgi to the plasma membrane. As the experimental approach described gave rise to a whole collection of CHO mutant cell lines characterized by a negative HASPB export phenotype, we hope to also identify mutants that are defective in early steps of HASPB biogenesis. The most important future goal will be to look for the defective genes by functional expression cloning and/or genome insertion analysis of the retrovirus used as a mutagen as well as to assign the corresponding gene products to defined steps of the HASPB biogenesis pathway on a functional basis.

We thank Britta Brügger (Heidelberg University Biochemistry Center) for critical comments on the manuscript. We would like to thank Lars Dietrich and Christian Ungermann (Heidelberg University Biochemistry Center) for many interesting discussions on protein acylation and SH4 domains. This study was supported by a grant of the German Research Council (DFG Ni 423/3-5).

References

Alce, T. M., Gokool, S., McGhie, D., Stager, S. and Smith, D. F. (1999). Expression of hydrophilic surface proteins in infective stages of Leishmania donovani. *Mol. Biochem. Parasitol.* **102**, 191-196.

Andrei, C., Dazzi, C., Lotti, L., Torrisi, M. R., Chimini, G. and Rubartelli, A. (1999). The secretory route of the leaderless protein interleukin 1beta involves exocytosis of endolysosome-related vesicles. *Mol. Biol. Cell* **10**, 1463-1475.

Andrei, C., Margiocco, P., Poggi, A., Lotti, L. V., Torrisi, M. R. and Rubartelli, A. (2004). Phospholipases C and A2 control lysosome-mediated IL-1 beta secretion: implications for inflammatory processes. *Proc. Natl. Acad. Sci. USA* **101**, 9745-9750.

Backhaus, R., Zehe, C., Wegehingel, S., Kehlenbach, A., Schwappach, B. and Nickel, W. (2004). Unconventional protein secretion: membrane translocation of FGF-2 does not require protein unfolding. *J. Cell Sci.* **117**, 1727-1736.

Bijlmakers, M. J. and Marsh, M. (1999). Trafficking of an acylated cytosolic protein: newly synthesized p56(lck) travels to the plasma membrane via the exocytic pathway. *J. Cell Biol.* **145**, 457-468.

Bijlmakers, M. J. and Marsh, M. (2003). The on-off story of protein palmitoylation. *Trends Cell Biol.* **13**, 32-42.

Cleves, A. E. (1997). Protein transports: the nonclassical ins and outs. *Curr. Biol.* **7**, R318-R320.

Cleves, A. E., Cooper, D. N., Barondes, S. H. and Kelly, R. B. (1996). A new pathway for protein export in Saccharomyces cerevisiae. *J. Cell Biol.* **133**, 1017-1026.

Cooper, D. N. and Barondes, S. H. (1990). Evidence for export of a muscle lectin from cytosol to extracellular matrix and for a novel secretory mechanism. *J. Cell Biol.* **110**, 1681-1691.

Denny, P. W., Gokool, S., Russell, D. G., Field, M. C. and Smith, D. F. (2000). Acylation-dependent protein export in Leishmania. *J. Biol. Chem.* **275**, 11017-11025.

Engling, A., Backhaus, R., Stegmayer, C., Zehe, C., Seelenmeyer, C., Kehlenbach, A., Schwappach, B., Wegehingel, S. and Nickel, W. (2002). Biosynthetic FGF-2 is targeted to non-lipid raft microdomains following translocation to the extracellular surface of CHO cells. *J. Cell Sci.* **115**, 3619-3631.

Fishburn, C. S., Herzmark, P., Morales, J. and Bourne, H. R. (1999). Gbetagamma and palmitate target newly synthesized Galphaz to the plasma membrane. *J. Biol. Chem.* **274**, 18793-18800.

Flieger, O., Engling, A., Bucala, R., Lue, H., Nickel, W. and Bernhagen, J. (2003). Regulated secretion of macrophage migration inhibitory factor is mediated by a non-classical pathway involving an ABC transporter. *FEBS Lett.* **551**, 78-86.

Flinn, H. M., Rangarajan, D. and Smith, D. F. (1994). Expression of a hydrophilic surface protein in infective stages of Leishmania major. *Mol. Biochem. Parasitol.* **65**, 259-270.

Florkiewicz, R. Z., Majack, R. A., Buechler, R. D. and Florkiewicz, E. (1995). Quantitative export of FGF-2 occurs through an alternative, energy-dependent, non-ER/Golgi pathway. *J. Cell Physiol.* **162**, 388-399.

Fujiki, Y., Hubbard, A. L., Fowler, S. and Lazarow, P. B. (1982). Isolation of intracellular membranes by means of sodium carbonate treatment: application to endoplasmic reticulum. *J. Cell Biol.* **93**, 97-102.

Futter, C. E., Gibson, A., Allchin, E. H., Maxwell, S., Ruddock, L. J., Odorizzi, G., Domingo, D., Trowbridge, I. S. and Hopkins, C. R. (1998). In polarized MDCK cells basolateral vesicles arise from clathrin-gamma-adaptin-coated domains on endosomal tubules. *J. Cell Biol.* **141**, 611-623.

Hughes, R. C. (1999). Secretion of the galectin family of mammalian carbohydrate-binding proteins. *Biochim. Biophys. Acta* **1473**, 172-185.

Jackson, A., Friedman, S., Zhan, X., Engleka, K. A., Forough, R. and Maciag, T. (1992). Heat shock induces the release of fibroblast growth factor 1 from NIH 3T3 cells. *Proc. Natl. Acad. Sci. USA* **89**, 10691-10695.

Jackson, A., Tarantini, F., Gamble, S., Friedman, S. and Maciag, T. (1995). The release of fibroblast growth factor-1 from NIH 3T3 cells in response to temperature involves the function of cysteine residues. *J. Biol. Chem.* **270**, 33-36.

Keenan, R. J., Freymann, D. M., Stroud, R. M. and Walter, P. (2001). The signal recognition particle. *Annu. Rev. Biochem.* **70**, 755-775.

Landriscina, M., Bagala, C., Mandinova, A., Soldi, R., Micucci, I., Bellum, S., Prudovsky, I. and Maciag, T. (2001a). Copper induces the assembly of a multiprotein aggregate implicated in the release of fibroblast growth factor 1 in response to stress. *J. Biol. Chem.* **276**, 25549-25557.

Landriscina, M., Soldi, R., Bagala, C., Micucci, I., Bellum, S., Tarantini, F., Prudovsky, I. and Maciag, T. (2001b). S100a13 participates in the release of fibroblast growth factor 1 in response to heat shock in vitro. *J. Biol. Chem.* **276**, 22544-22552.

LaVallee, T. M., Tarantini, F., Gamble, S., Carreira, C. M., Jackson, A. and Maciag, T. (1998). Synaptotagmin-1 is required for fibroblast growth factor-1 release. *J. Biol. Chem.* **273**, 22217-22223.

Lippincott-Schwartz, J., Yuan, L. C., Bonifacino, J. S. and Klausner, R. D. (1989). Rapid redistribution of Golgi proteins into the ER in cells treated with Brefeldin A: evidence for membrane cycling from Golgi to ER. *Cell* **56**, 801-813.

Liu, X., Constantinescu, S. N., Sun, Y., Bogan, J. S., Hirsch, D., Weinberg, R. A. and Lodish, H. F. (2000). Generation of mammalian cells stably expressing multiple genes at predetermined levels. *Anal. Biochem.* **280**, 20-28.

Lutomski, D., Fouillit, M., Bourin, P., Mellottee, D., Denize, N., Pontet, M., Bladier, D., Caron, M. and Joubert-Caron, R. (1997). Externalization and binding of galectin-1 on cell surface of K562 cells upon erythroid differentiation. *Glycobiology* **7**, 1193-1199.

Mandinova, A., Soldi, R., Graziani, I., Bagala, C., Bellum, S., Landriscina, M., Tarantini, F., Prudovsky, I. and Maciag, T. (2003). S100A13 mediates the copper-dependent stress-induced release of IL-1alpha from both human U937 and murine NIH 3T3 cells. *J. Cell Sci.* **116**, 2687-2696.

McKean, P. G., Trenholme, K. R., Rangarajan, D., Keen, J. K. and Smith, D. F. (1997). Diversity in repeat-containing surface proteins of Leishmania major. *Mol. Biochem. Parasitol.* **86**, 225-235.

McKean, P. G., Denny, P. W., Knuepfer, E., Keen, J. K. and Smith, D. F. (2001). Phenotypic changes associated with deletion and overexpression of a stage-regulated gene family in Leishmania. *Cell. Microbiol.* **3**, 511-523.

Mignatti, P. and Rifkin, D. B. (1991). Release of basic fibroblast growth factor, an angiogenic factor devoid of secretory signal sequence: a trivial phenomenon or a novel secretion mechanism? *J. Cell. Biochem.* **47**, 201-207.

Mignatti, P., Morimoto, T. and Rifkin, D. B. (1992). Basic fibroblast growth factor, a protein devoid of secretory signal sequence, is released by cells via a pathway independent of the endoplasmic reticulum-Golgi complex. *J. Cell Physiol.* **151**, 81-93.

Misumi, Y., Miki, A., Takatsuki, A., Tamura, G. and Ikehara, Y. (1986). Novel blockade by brefeldin A of intracellular transport of secretory proteins in cultured rat hepatocytes. *J. Biol. Chem.* **261**, 11398-11403.

Muesch, A., Hartmann, E., Rohde, K., Rubartelli, A., Sitia, R. and Rapoport, T. A. (1990). A novel pathway for secretory proteins? *Trends Biochem. Sci.* **15**, 86-88.

Nakamura, N., Rabouille, C., Watson, R., Nilsson, T., Hui, N., Slusarewicz, P., Kreis, T. E. and Warren, G. (1995). Characterization of a cis-Golgi matrix protein, GM130. *J. Cell Biol.* **131**, 1715-1726.

Nickel, W. (2003). The mystery of nonclassical protein secretion. *Eur. J. Biochem.* **270**, 2109-2119.

Nickel, W., Brügger, B. and Wieland, F. T. (2002). Vesicular transport: the core machinery of COPI recruitment and budding. *J. Cell Sci.* **115**, 3235-3240.

Orci, L., Tagaya, M., Amherdt, M., Perrelet, A., Donaldson, J. G., Lippincott-Schwartz, J., Klausner, R. D. and Rothman, J. E. (1991). Brefeldin A, a drug that blocks secretion, prevents the assembly of non-clathrin-coated buds on Golgi cisternae. *Cell* **64**, 1183-1195.

Palade, G. (1975). Intracellular aspects of the process of protein synthesis. *Science* **189**, 347-358.

Pimenta, P. F., Pinto da Silva, P., Rangarajan, D., Smith, D. F. and Sacks, D. L. (1994). Leishmania major: association of the differentially expressed gene B protein and the surface lipophosphoglycan as revealed by membrane capping. *Exp. Parasitol.* **79**, 468-479.

Prudovsky, I., Bagala, C., Tarantini, F., Mandinova, A., Soldi, R., Bellum, S. and Maciag, T. (2002). The intracellular translocation of the components of the fibroblast growth factor 1 release complex precedes their assembly prior to export. *J. Cell Biol.* **158**, 201-208.

Prudovsky, I., Mandinova, A., Soldi, R., Bagala, C., Graziani, I., Landriscina, M., Tarantini, F., Duarte, M., Bellum, S., Doherty, H. et al. (2003). The non-classical export routes: FGF1 and IL-1{alpha} point the way. *J. Cell Sci.* **116**, 4871-4881.

Rangarajan, D., Gokool, S., McCrossan, M. V. and Smith, D. F. (1995). The gene B protein localises to the surface of Leishmania major parasites in the absence of metacyclic stage lipophosphoglycan. *J. Cell Sci.* **108**, 3359-3366.

Rothman, J. E. (1994). Mechanisms of intracellular protein transport. *Nature* **372**, 55-63.

Rothman, J. E. and Wieland, F. T. (1996). Protein sorting by transport vesicles. *Science* **272**, 227-234.

Rubartelli, A. and Sitia, R. (1991). Interleukin 1 beta and thioredoxin are secreted through a novel pathway of secretion. *Biochem. Soc. Trans.* **19**, 255-259.

Rubartelli, A., Cozzolino, F., Talio, M. and Sitia, R. (1990). A novel secretory pathway for interleukin-1 beta, a protein lacking a signal sequence. *EMBO J.* **9**, 1503-1510.

Schäfer, T., Zentgraf, H., Zehe, C., Brügger, B., Bernhagen, J. and Nickel, W. (2004). Unconventional secretion of fibroblast growth factor 2 is mediated by direct translocation across the plasma membrane of mammalian cells. *J. Biol. Chem.* **279**, 6244-6251.

Seelenmeyer, C., Wegehingel, S., Lechner, J. and Nickel, W. (2003). The cancer antigen CA125 represents a novel counter receptor for galectin-1. *J. Cell Sci.* **116**, 1305-1318.

Shin, J. T., Opalenik, S. R., Wehby, J. N., Mahesh, V. K., Jackson, A., Tarantini, F., Maciag, T. and Thompson, J. A. (1996). Serum-starvation induces the extracellular appearance of FGF-1. *Biochim. Biophys. Acta* **1312**, 27-38.

Tarantini, F., LaVallee, T., Jackson, A., Gamble, S., Carreira, C. M., Garfinkel, S., Burgess, W. H. and Maciag, T. (1998). The extravesicular domain of synaptotagmin-1 is released with the latent fibroblast growth factor-1 homodimer in response to heat shock. *J. Biol. Chem.* **273**, 22209-22216.

Trudel, C., Faure-Desire, V., Florkiewicz, R. Z. and Baird, A. (2000). Translocation of FGF2 to the cell surface without release into conditioned media. *J. Cell Physiol.* **185**, 260-268.

van't Hof, W. and Resh, M. D. (1997). Rapid plasma membrane anchoring of newly synthesized p59fyn: selective requirement for NH2-terminal myristoylation and palmitoylation at cysteine-3. *J. Cell Biol.* **136**, 1023-1035.